Angular Lens

Rishabh Sahu[1,†], Swati Chaudhary[1,†,#], Kedar Khare[2], Mishkatul
Bhattacharya[3], Harshawardhan Wanare[1], and Anand Kumar Jha[1*]

[1] Department of Physics, Indian Institute of Technology Kanpur, Kanpur, UP 208016, India
[2] Department of Physics, Indian Institute of Technology Delhi, Hauz Khas, New Delhi 110016, India
[3] School of Physics and Astronomy, Rochester Institute of Technology, Rochester, New York 14623, USA

(Dated: November 10, 2017)

We propose a single phase-only optical element that transforms different orbital angular momentum (OAM) modes into localized spots at separated angular positions on a transverse plane. We refer to this element as an angular lens since it separates out OAM modes in a manner analogous to how a converging lens separates out transverse wave-vector modes at the focal plane. We also simulate the proposed angular lens using a spatial light modulator and experimentally demonstrate its working. Our work can have important implications for OAM-based classical and quantum communication applications.

It is known that the transverse position and the transverse wave-vector bases form a two-dimensional Fourier transform pair and that a converging lens is a phase-only optical element that performs this Fourier transformation [1, 2]. Owing to this transformation property of a lens, optical modes characterized by different transverse wave-vectors get mapped onto separated localized spots on a transverse plane after passing through a lens. When the aperture-size of the lens is infinite, the localized spots take the form of two-dimensional Dirac-delta functions and the wave-vector separation is said to be perfect. However, with a finite aperture-size lens, this separation is imperfect and its degree characterizes the resolving power of the lens.

It is now also known that optical modes having an $e^{-i\ell\phi}$ phase profile can carry $\ell\hbar$ orbital angular momentum (OAM) per photon [3]. Here ϕ is the angular position and ℓ is referred to as the aziumthal mode index or the OAM mode index. This feature of OAM modes has made them extremely important for communication and computation protocols, in terms of system capacity [4–6], security [7–9], transmission bandwidth [10, 11], gate implementations [12, 13], supersensitive measurements [14] and fundamental tests of quantum mechanics [15–18]. However, one major challenge in implementing OAM-based protocols is the efficient separation and detection of OAM-modes. The earliest efforts at separating OAM modes were based on using a phase-only hologram, either thin [19, 20] or thick [21]. But these methods turned out to be quite inefficient and are not suitable at single photon levels. Later, techniques based on concatenated Mach-Zehnder interferometers [22, 23] and rotational Doppler shift were proposed [24, 25]. Although these techniques are in principle 100% efficient even at the single-photon level, it is extremely difficult to implement them for more than a few modes. More recently, there have been efforts [26, 27] based on log-polar mapping [28, 29] that can work with more modes and also at the single-photon level. However, these recent methods involve several elements and are quite cumbersome
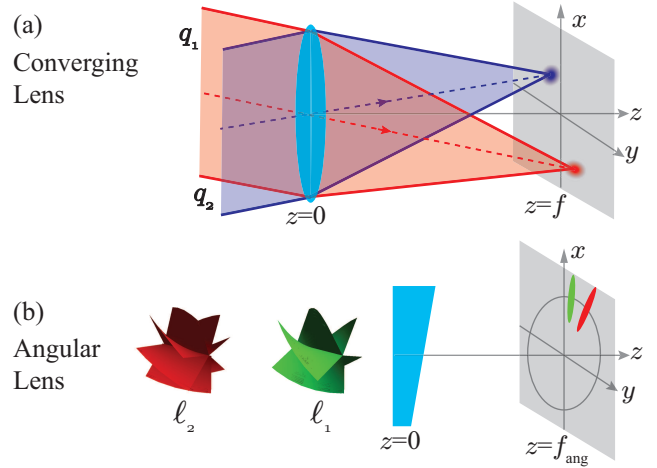

FIG. 1: (a) Working of a converging lens. The transverse wave-vector modes $\boldsymbol{q}_1$ and $\boldsymbol{q}_2$ with phase profiles $e^{i\boldsymbol{q}_1\cdot\boldsymbol{\rho}}$ and $e^{i\boldsymbol{q}_2\cdot\boldsymbol{\rho}}$ get localized at separate spatial locations. (b) Illustrating the expected working of an angular lens. The OAM modes ℓ_1 and ℓ_2 with phase profiles $e^{-i\ell_1\phi}$ and $e^{-i\ell_2\phi}$ get localized at separate angular positions.

for optical fields containing several OAM modes. Therefore, the existing methods for separating out OAM modes are either inefficient or unsuitable at single-photon levels, or involve multiple elements for their implementation.

In this letter, we propose and demonstrate a single phase-only optical element that separates out OAM modes into localized spots in much the same way as a converging lens separates out transverse wave-vector modes. We refer to this element as an "angular lens" and show that it provides a natural way of separating out OAM modes and can not only work with a large number of incoming modes but also at the single-photon level.

Figure 1(a) illustrates how a converging lens separates out different transverse wave-vector modes. The phase transformation function $T(x, y)$ of a thin converging lens within the paraxial approximation is given by (see Section 5.2 of Ref. [1]): $T(x, y) = \exp[-\frac{ik}{2f}(x^2 + y^2)]$, where

f is the focal length of the lens and where $k = 2\pi/\lambda$ with λ being the wavelength of light. The lens transforms the transverse wave-vector modes $\boldsymbol{q}_1$ and $\boldsymbol{q}_2$ with phase profiles $e^{i\boldsymbol{q}_1 \cdot \boldsymbol{\rho}}$ and $e^{i\boldsymbol{q}_2 \cdot \boldsymbol{\rho}}$, where $|\boldsymbol{q}_1|, |\boldsymbol{q}_2| \ll k$, into localized spots on a transverse plane kept at $z = f$. Figure 1(b) depicts expected analogous working of an angular lens. We now want to find out the phase transformation function of such a lens. We begin by noting that the angular-position and the orbital angular momentum (OAM) bases form a Fourier transform pair in much the same way as the transverse position and transverse wave-vector bases do [30–32]. Therefore, it is natural to expect the transformation function of an angular lens to have a quadratic dependence on ϕ just as the transformation function of a converging lens has quadratic dependences on x and y. However, unlike the transverse position coordinates (x, y) the cylindrical coordinates (ρ, ϕ) do not form a two-dimensional Fourier pair. Therefore, it is not straightforward to arrive at an analogous functional dependence on ρ. Nevertheless, we take a hint from Ref. [33], in which it was shown that an axicon, which has a transformation function given by $e^{i\beta\rho}$ with β being a constant, transforms a Laguerre-Gaussian mode into an ultranarrow annulus. With this hint, we take the following as the transformation function $T_{\text{ang}}(\rho, \phi)$ of our proposed angular lens:

$$T_{\text{ang}}(\rho, \phi) = \exp\left[-i(\alpha\phi^2 - \beta\rho)\right]. \quad (1)$$

Here α, β are two constants and $\phi \in [-\pi, \pi]$ and $\rho \in [0, \infty]$. The thickness function corresponding to the phase transformation function has been plotted in Fig. 2 (a).

Let us consider the experimental situation shown in Fig.2 (b). An angular lens with the transformation function given by Eq. (1) is placed at $z = 0$ and an input field with amplitude $E_{z=0}(\rho', \phi')$ at $z = 0$ is incident on it. The field amplitude $E_{z=z}(\rho, \phi)$ at z is given by the Fresnel diffraction integral [1]:

$$E_{z=z}(\rho, \phi) = \frac{e^{ikz}}{i\lambda z} e^{i\frac{k}{2z}\rho^2} \int_0^\infty \int_0^{2\pi} E_{z=0}(\rho', \phi')$$

$$\times e^{-i(\alpha\phi'^2 - \beta\rho')} e^{i\frac{k}{2z}\rho'^2} e^{-i\frac{k\rho\rho'}{z}\cos(\phi - \phi')} \rho' d\rho' d\phi'. \quad (2)$$

First of all we investigate the transformation properties of our angular lens for input field modes given by $E_{z=0}(\rho', \phi') = e^{-i\ell\phi'}$. Such modes have constant transverse intensity at $z = 0$. In our experiment, we generate these modes by first expanding our continuous-wave He-Ne laser beam to be 1-cm wide. We then diffract this laser beam from the spatial light modulator (SLM) kept at $z = 0$ after putting an appropriate phase pattern on it [19]. We also put a circular aperture of diameter $D = 2$ mm onto the SLM so that only a small circular portion of the incoming laser beam undergoes diffraction and thus, to a good approximation, the intensity in the
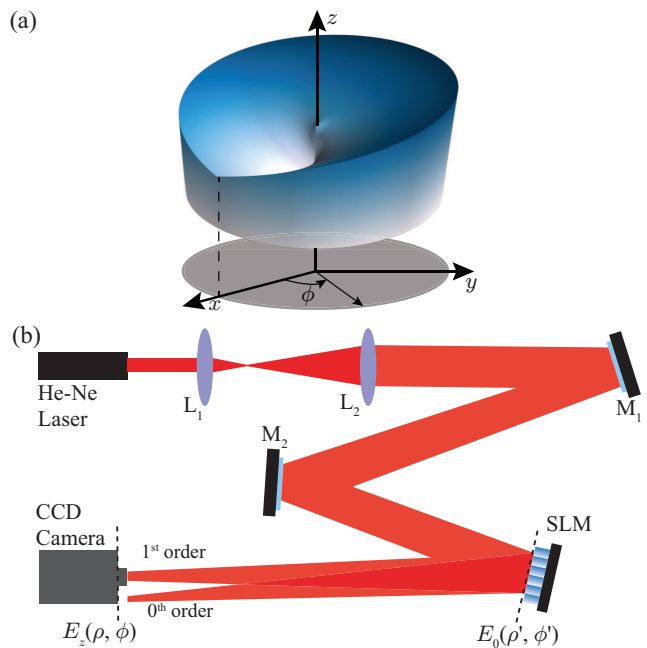

FIG. 2: (a) The thickness function of the proposed angular lens. (b) The experimental Setup. SLM is spatial light modulator, L stands for a converging lens, and M stands for a mirror.

circular portion can be taken as constant. The transformation function corresponding to the angular lens at $z = 0$ is also simulated using the same SLM and α and β are electronically changed in order to simulate different lenses. By changing ℓ in a sequential manner, we generate a range of OAM modes. The transformation properties of the lens is studied by recording the transverse intensity at the first SLM diffraction order using a CCD camera placed at z.

Figure 3 shows the combined intensity patterns observed by the CCD camera kept at $z = 65$ cm for a range of OAM modes with various ℓ and with separation $\Delta\ell$. Figures 3 (a), (b), and (c) show the combined intensity patterns corresponding to α equal to 3, 8, and 16, respectively. In order to consider the two modes as separated we adapt the following resolution criterion: if in the combined two-dimensional intensity plot at z, the ratio of the intensity at the minimum located in between the two maxima and that at the maxima is less than about 0.3 then the two modes are resolved. This criterion is much stringent than that of Rayleigh, which allows for ratios up to 0.811. The value of β was optimized to satisfy the above criterion, and for the three α values β was found to be 17.7 mm^{-1}, 29.9 mm^{-1}, and 49.2 mm^{-1}, respectively. We find that different OAM modes get transformed into diffraction patterns localized at separate angular positions and that as α increases the mode separation $\Delta\ell$ that could be resolved increases as well. For the three α values, we find that modes with separation $\Delta\ell$ equal to
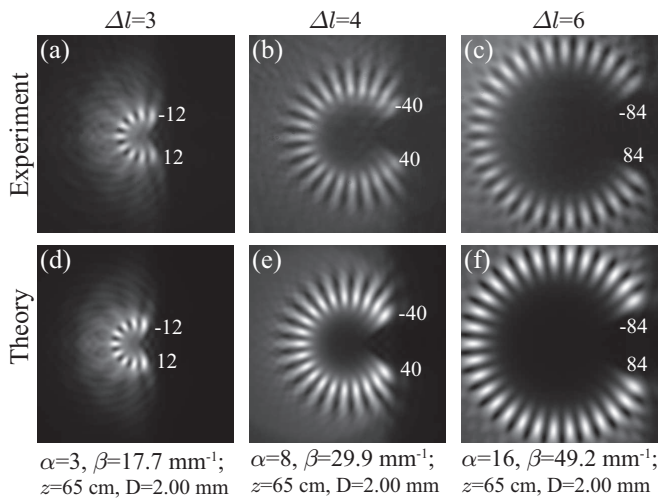
FIG. 3: Transformation of constant-intensity OAM modes by the angular lens. (a), (b), and (c) are the combined intensity patterns for various ℓ observed at $z = 65$ cm. (d)-(f) are the corresponding theoretically expected patterns obtained by numerically solving Eq. (2). The screen size in all the above plots is 6.27 mm × 6.27 mm.
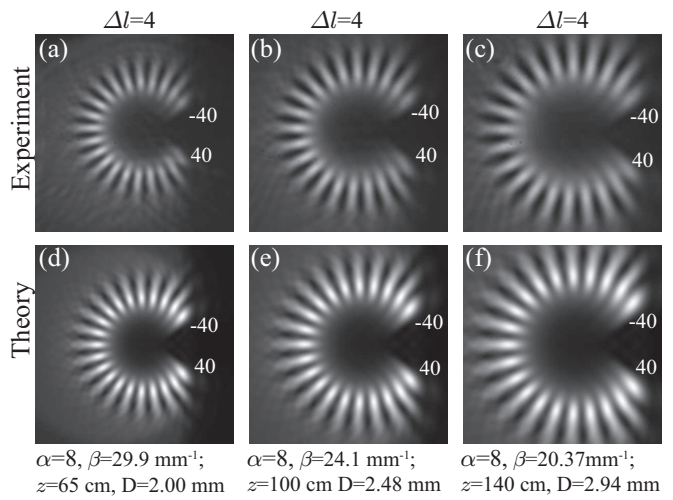

FIG. 4: Scaling of diffraction patterns with z. (a), (b), and (c) are the combined intensity patterns observed at three z values. (d)-(f) are the theoretically expected diffraction patterns. The screen size in all the above plots is 6.27 mm × 6.27 mm.

3, 4, and 6 could be resolved. Further, we find that as α increases, the range of modes that can be transformed into localized functions also increases. Figures 3 (d)-(f) show the corresponding theoretical diffraction patterns as obtained by numerically solving Eq. (2) for the same set of parameters.

In a converging lens the resolving power is decided by the size of the lens. In our proposed angular lens, it seems that α is playing an analogous role. Another important feature of a converging lens is that for a given input field the focal intensity patterns due to lenses with different focal lengths remain the same except for an overall scaling of the pattern. The proposed angular lens also shows an analogous scaling property for fixed α values. In order to show this, let us consider two angular lenses with the same α but with β parameters being equal to β_1 and β_2 and the aperture size D being equal to D_1 and D_2, respectively. Let us assume that with β_1 and D_1 the angular lens produces the optimized diffraction pattern at $z = z_1$. The field amplitude $E_{z=z_1}^{(1)}(\rho, \phi)$ in this case can be written using Eq. (2) as

$$E_{z=z_1}^{(1)}(\rho, \phi) = \frac{e^{ikz_1}}{i\lambda z_1} e^{i\frac{k}{2z_1}\rho^2} \int_0^{D_1/2} \int_0^{2\pi} E_{z=0}(\phi')$$
$$\times e^{-i(\alpha\phi'^2 - \beta_1\rho')} e^{i\frac{k}{2z_1}\rho'^2} e^{-i\frac{k\rho\rho'}{z_1}\cos(\phi-\phi')} \rho' d\rho' d\phi'. \quad (3)$$

We at once see that since the input field amplitude depends only on ϕ' the functional form of the intensity due to the first angular lens at z_1 is equal to that due to the second lens at z_2, that is, $|E_{z=z_2}^{(2)}(\rho, \phi)|^2 =$ $|E_{z=z_1}^{(1)}(\rho/a, \phi)|^2$, if

$$z_2 = a^2 z_1, \ \beta_2 = \frac{\beta}{a} \text{ and } D_2 = \frac{D_1}{a}, \quad (4)$$

for a given constant value of a. Figure 4 shows the experimental and theoretical results illustrating this analogous focusing property of the angular lens. The diffraction pattern in Fig. 4 (a) is for a lens with $\alpha = 8$ and $D = 2$ mm, and the β parameter was optimized in order to satisfy our resolution criterion. For the results in Fig. 4 (b) and (c), we chose z to be 100 cm and 140 cm respectively and the corresponding β and the size of the lens were chosen simply using the scaling in Eq. (4) without any optimization. Figure 4 (d)-(f) are the theory patterns obtained by numerically solving Eq. (2) for the same set of parameters.

Next, we study how our angular lens performs for the Laguerre-Gaussian (LG) modes, which are the exact propagating solutions of the paraxial Helmholtz equation and are denoted by two indices, ℓ and p. The index ℓ decides the OAM content and the index p decides the radial intensity distribution. We produce LG modes using the method by Arrizón et al. [34]. Figure 5 shows the combined intensity patterns observed by the CCD camera kept at $z = 100$ cm when a range of LG modes with $p = 0$ and with separation $\Delta\ell$ were sequentially incident on angular lenses having various sets of values for α and β. Figures 5 (a), (b), and (c) show the combined intensity patterns corresponding to α being equal to 7, 16, and 30, respectively. As before, for a given value of α, the value of β was optimized to satisfy our resolution criterion. The values of β for the three α values were found to be 27.0 mm^{-1}, 36.5 mm^{-1}, and 51.0 mm^{-1}, respectively.

The mode separation $\Delta\ell$ that could be resolved for the three α values, were 4, 5, and 6, respectively. Figures 5 (d)-(f) show the theoretically expected diffraction patterns obtained by numerically solving Eq. (2). Although the proposed angular lens is able to separate out the LG modes, it does not have all the analogous feature as in the case of flat-intensity OAM modes. More specifically, we do not see the same scaling as is seen in the case of constant-intensity OAM modes through Eq. (3) and Eq. (4). This is because in this case the input field amplitude depends on both ρ' and ϕ' and therefore Eq. (3) does not show the same scaling.

In conclusion, we have proposed a single phase-only optical element that can transform different OAM modes into localized patterns at separated angular positions on a transverse plane. Using an SLM, we have experimentally demonstrated the working of our proposed angular lens for two different types of OAM modes. For constant-intensity OAM modes, our angular lens works in a manner analogous to how a converging lens works for transverse wave-vector modes. Even for the LG modes, our proposed angular lens is able to separate out the modes based on their OAM mode index. Although our proposed angular lens in this paper does not have perfect resolving power, in several situations there are techniques that are employed to increase the resolving power of an optical element beyond its usual diffraction limit. For example, in the context of log-polar mapping based method [26, 27, 35, 36], which does not have perfect resolving power, it was shown that when the method is used in combination with the idea of beam copying [37] it can achieve perfect resolution [35, 36]. We believe that similar techniques can also enhance the resolving power of
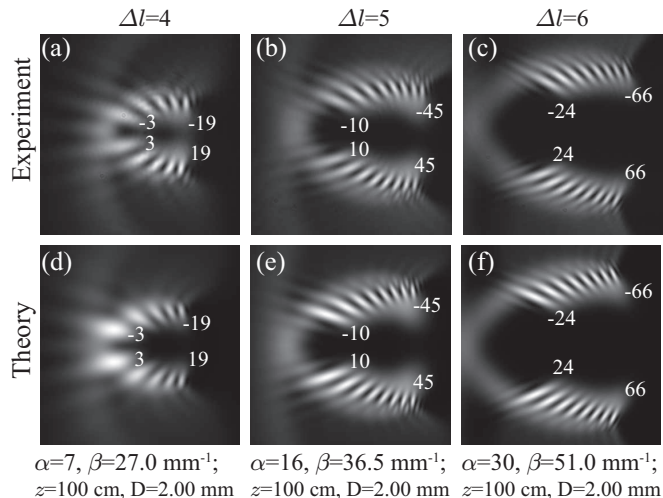
our angular lens beyond its diffraction limit. Since the proposed angular lens is purely a phase-only element and works at any light level, we expect our work to have several important implications for OAM-based communication protocols in both classical [4–6] and quantum domains [7–18].

––––––––––––

* Electronic address: akjha9@gmail.com ; # Presently at California Institute of Technology, Pasadena, CA, USA; † Both the authors contibuted equally to the work

[1] J. Goodman, *Introduction to Fourier Optics*, 2nd ed. (McGraw Hill, New York, 1996).

[2] M. Born and E. Wolf, *Principles of Optics*, 7th expanded ed. (Cambridge University Press, Cambridge, 1999).

[3] L. Allen, M. W. Beijersbergen, R. J. C. Spreeuw, and J. P. Woerdman, Phys. Rev. A **45**, 8185 (1992).

[4] J. Wang, J.-Y. Yang, I. M. Fazal, N. Ahmed, Y. Yan, H. Huang, Y. Ren, Y. Yue, S. Dolinar, M. Tur, and A. E. Willner, Nat Photon **6**, 488 (2012).

[5] N. Bozinovic, Y. Yue, Y. Ren, M. Tur, P. Kristensen, H. Huang, A. E. Willner, and S. Ramachandran, Science **340**, 1545 (2013).

[6] Y. Yan, G. Xie, M. P. J. Lavery, H. Huang, N. Ahmed, C. Bao, Y. Ren, Y. Cao, L. Li, Z. Zhao, A. F. Molisch, M. Tur, M. J. Padgett, and A. E. Willner, Nature Communications **5**, 4876 (2014).

[7] V. Karimipour, A. Bahraminasab, and S. Bagherinezhad, Phys. Rev. A **65**, 052331 (2002).

[8] N. J. Cerf, M. Bourennane, A. Karlsson, and N. Gisin, Phys. Rev. Lett. **88**, 127902 (2002).

[9] G. M. Nikolopoulos, K. S. Ranade, and G. Alber, Phys. Rev. A **73**, 032325 (2006).

[10] M. Fujiwara, M. Takeoka, J. Mizuno, and M. Sasaki, Phys. Rev. Lett. **90**, 167906 (2003).

[11] J. Cortese, Phys. Rev. A **69**, 022302 (2004).

[12] T. C. Ralph, K. J. Resch, and A. Gilchrist, Phys. Rev. A **75**, 022313 (2007).

[13] B. P. Lanyon, M. Barbieri, M. P. Almeida, T. Jennewein, T. C. Ralph, K. J. Resch, G. J. Pryde, J. L. O/'Brien, A. Gilchrist, and A. G. White, Nat Phys **5**, 134 (2009).

[14] A. K. Jha, G. S. Agarwal, and R. W. Boyd, Phys. Rev. A **83**, 053829 (2011).

[15] D. Kaszlikowski, P. Gnaciński, M. Żukowski, W. Miklaszewski, and A. Zeilinger, Phys. Rev. Lett. **85**, 4418 (2000).

[16] D. Collins, N. Gisin, N. Linden, S. Massar, and S. Popescu, Phys. Rev. Lett. **88**, 040404 (2002).

[17] T. Vértesi, S. Pironio, and N. Brunner, Phys. Rev. Lett. **104**, 060401 (2010).

[18] J. Leach, B. Jack, J. Romero, M. Ritsch-Marte, R. W. Boyd, A. K. Jha, S. M. Barnett, S. Franke-Arnold, and

| | Δl=4 | Δl=5 | Δl=6 |

α=7, β=27.0 mm^{-1}; z=100 cm, D=2.00 mm $\quad$ α=16, β=36.5 mm^{-1}; z=100 cm, D=2.00 mm $\quad$ α=30, β=51.0 mm^{-1}; z=100 cm, D=2.00 mm

FIG. 5: Transformation of LG modes by the proposed angular lens. (a), (b), and (c) are the combined intensity patterns for various ℓ observed at $z = 100$ cm. (d)-(f) are the theoretically expected diffraction patterns. The screen size in all the above plots is 5.63 mm × 5.63 mm.

M. J. Padgett, Opt. Express **17**, 8287 (2009).

[19] A. Mair, A. Vaziri, G. Weihs, and A. Zeilinger, Nature **412**, 313 (2001).

[20] G. Gibson, J. Courtial, M. J. Padgett, M. Vasnetsov, V. Pas'ko, S. M. Barnett, and S. Franke-Arnold, Opt. Express **12**, 5448 (2004).

[21] M. T. Gruneisen, R. C. Dymale, K. E. Stoltenberg, and N. Steinhoff, New Journal of Physics **13**, 083030 (2011).

[22] J. Leach, M. J. Padgett, S. M. Barnett, S. Franke-Arnold, and J. Courtial, Phys. Rev. Lett. **88**, 257901 (2002).

[23] J. Leach, J. Courtial, K. Skeldon, S. M. Barnett, S. Franke-Arnold, and M. J. Padgett, Phys. Rev. Lett. **92**, 013601 (2004).

[24] M. Vasnetsov, J. Torres, D. Petrov, and L. Torner, Optics letters **28**, 2285 (2003).

[25] J. Courtial, D. A. Robertson, K. Dholakia, L. Allen, and M. J. Padgett, Phys. Rev. Lett. **81**, 4828 (1998).

[26] G. C. Berkhout, M. P. Lavery, J. Courtial, M. W. Beijersbergen, and M. J. Padgett, Phys. Rev. Lett. **105**, 153601 (2010).

[27] M. P. Lavery, D. J. Robertson, G. C. Berkhout, G. D. Love, M. J. Padgett, and J. Courtial, Optics express **20**,

2110 (2012).

[28] O. Bryngdahl, JOSA **64**, 1092 (1974).

[29] O. Bryngdahl, Optics Communications **10**, 164 (1974).

[30] E. Yao, S. Franke-Arnold, J. Courtial, S. Barnett, and M. Padgett, Opt. Express **14**, 9071 (2006).

[31] A. K. Jha, B. Jack, E. Yao, J. Leach, R. W. Boyd, G. S. Buller, S. M. Barnett, S. Franke-Arnold, and M. J. Padgett, Phys. Rev. A **78**, 043810 (2008).

[32] A. K. Jha, J. Leach, B. Jack, S. Franke-Arnold, S. M. Barnett, R. W. Boyd, and M. J. Padgett, Phys. Rev. Lett. **104**, 010501 (2010).

[33] J. Arlt, R. Kuhn, and K. Dholakia, journal of modern optics **48**, 783 (2001).

[34] V. Arrizón, U. Ruiz, R. Carrada, and L. A. González, J. Opt. Soc. Am. A **24**, 3500 (2007).

[35] M. N. OSullivan, M. Mirhosseini, M. Malik, and R. W. Boyd, Optics express **20**, 24444 (2012).

[36] M. Mirhosseini, M. Malik, Z. Shi, and R. W. Boyd, Nature communications **4**, (2013).

[37] L. A. Romero and F. M. Dickey, JOSA A **24**, 2280 (2007).